NEURAL REGENERATION RESEARCH
October 2016, Volume 11, Issue 10
www.nrronline.org

RESEARCH ARTICLE

Human amniotic epithelial cells combined with silk fibroin scaffold in the repair of spinal cord injury

Ting-gang Wang[1], Jie Xu[2], Ai-hua Zhu[2], Hua Lu[2], Zong-ning Miao[2], Peng Zhao[2], Guo-zhen Hui[3], Wei-jiang Wu[2,*]

1 Department of Neurology, Wuxi Third People's Hospital, Wuxi, Jiangsu Province, China
2 Department of Neurosurgery, Wuxi Third People's Hospital, Wuxi, Jiangsu Province, China
3 First Affiliated Hospital, Soochow University, Suzhou, Jiangsu Province, China

How to cite this article: *Wang TG, Xu J, Zhu AH, Lu H, Miao ZN, Zhao P, Hui GZ, Wu WJ (2016) Human amniotic epithelial cells combined with silk fibroin scaffold in the repair of spinal cord injury. Neural Regen Res 11(10):1670-1677.*

Funding: *This research was supported by the Scientific Research Project Fund of Wuxi Municipal Health and Family Planning Commission, No. MS201402.*

Graphical Abstract

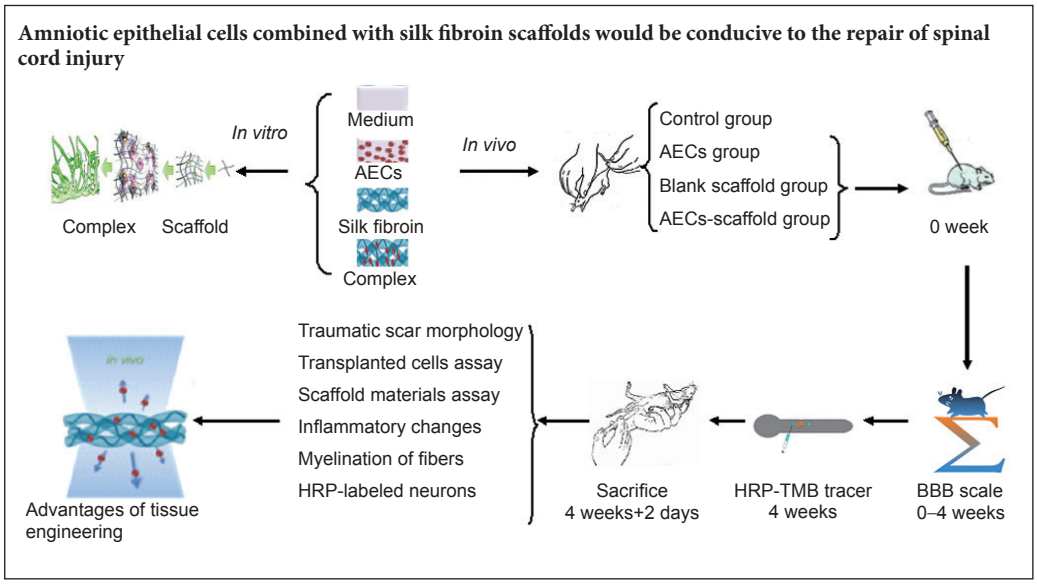

***Correspondence to:**
Wei-jiang Wu, M.D., wuwj2004@sohu.com.

orcid:
0000-0003-0147-3099 (Wei-jiang Wu)

doi: *10.4103/1673-5374.193249*

Accepted: *2016-08-22*

Abstract

Treatment and functional reconstruction after central nervous system injury is a major medical and social challenge. An increasing number of researchers are attempting to use neural stem cells combined with artificial scaffold materials, such as fibroin, for nerve repair. However, such approaches are challenged by ethical and practical issues. Amniotic tissue, a clinical waste product, is abundant, and amniotic epithelial cells are pluripotent, have low immunogenicity, and are not the subject of ethical debate. We hypothesized that amniotic epithelial cells combined with silk fibroin scaffolds would be conducive to the repair of spinal cord injury. To test this, we isolated and cultured amniotic epithelial cells, and constructed complexes of these cells and silk fibroin scaffolds. Implantation of the cell-scaffold complex into a rat model of spinal cord injury resulted in a smaller glial scar in the damaged cord tissue than in model rats that received a blank scaffold, or amniotic epithelial cells alone. In addition to a milder local immunological reaction, the rats showed less inflammatory cell infiltration at the transplant site, milder host-versus-graft reaction, and a marked improvement in motor function. These findings confirm that the transplantation of amniotic epithelial cells combined with silk fibroin scaffold can promote the repair of spinal cord injury. Silk fibroin scaffold can provide a good nerve regeneration microenvironment for amniotic epithelial cells.

Key Words: *nerve regeneration; spinal cord injury; amniotic epithelial cells; silk fibroin; scaffold; transplantation; glial scar; microenvironment; immunological reaction; rejection; neural regeneration*

Introduction

Although the central nervous system has some regenerative capacity, a glial scar is formed during self repair, which hinders axonal growth and blood vessel ingrowth (Lee-Liu, 2013; Khankan, 2015). Implanting a suitable matrix material in the lesion, such as a hydrogel, helps to guide the growth of axons and blood vessels (Chow, 2007; van Neerven, 2014), strengthen the migration of regenerating cells, and control glial scar formation.

Research into the application of tissue engineering technology in central nervous system repair is still in its infancy. Hydrogels are the most commonly used matrix materials in transplantation research (Jgamadze, 2015; Karumbaiah, 2015; Min, 2015; Rivet et al., 2015; Li et al., 2016). Using three-dimensional printing technology to build cell carriers has been proposed as a direction of future research (Dingle, 2015; Hopkins, 2015; Hsieh, 2015). However, silk fibroin, a natural material (Meinel et al., 2005; Marsano et al., 2008; Ghezzi et al., 2011), has better biocompatibility, biodegradability, and plasticity than synthetic materials (Tang, 2009; Zhao, 2013). *In vitro* experiments also confirmed that it was more conducive to cell culture and amplification (Arkhipova, 2016; Woloszyk, 2016). Silk fibroin is eventually expected to be applied in the clinic for the treatment of central nervous system damage and degenerative diseases, particularly when combining suitable pluripotent seed cells to construct tissue-engineered materials.

The combined use of neural stem cells and artificial scaffold materials is becoming more popular in investigations of central nervous system injury (Binan et al., 2015; Taylor et al., 2015; Wang et al., 2015; Zhu et al., 2015), but such experiments face challenges such as ethical issues and histocompatibility problems. However, the human amniotic membrane provides another source of suitable cells and, being a clinical waste product, it is abundant. Amniotic epithelial cells (AECs) have multiple differentiation potentials, are non-neoplastic, and have low immunogenicity, in addition to avoiding the ethical challenges of other materials (Gao et al., 2012; Corradetti et al., 2013; Rutigliano et al., 2013; Gramignoli et al., 2016). Indeed, AECs might be the ideal seed cells, constituting the perfect central nervous system repair material when combined with a natural scaffold material such as silk fibroin.

Materials and Methods

Human amniotic membrane

Healthy full-term placenta was obtained from women who had undergone a cesarean section at the Third People's Hospital of Wuxi City, China, with informed consent. Human AECs were isolated from the placenta and cultured as described below. The study was approved by the local research ethics committee.

Inclusion criterion: Healthy full-term pregnant women.

Exclusion criteria: Hepatitis and human immunodeficiency virus (HIV)-positive puerpera; over 40 weeks of pregnancy.

All experimental procedures followed the *International Ethical Guidelines for Biomedical Research Involving Human Subjects*, developed by the World Health Organization in 2002.

Animals

Thirty-two clean adult female Sprague-Dawley rats, weighing 250–300 g, were provided by the Laboratory Animal Center of Soochow University, China (license No. SCXK (Su) 2013-0009) and housed at the Model Animal Research Center, Schistosomiasis Control and Research Institute, Jiangsu Province, China. All protocols were performed in accordance with *Regulations on the Management of Laboratory Animals*, and the *Laboratory Animal Management Guidelines of Soochow University, China*.

Thirty-two rats were randomly assigned to four groups: control (n = 6), blank scaffold (SCI + scaffold) (n = 6), AECs (SCI + AECs) (n = 10) and AECs-scaffold (SCI + AECs-scaffold) (n = 10).

Isolation and culture of AECs *in vitro*

Samples of placenta (15 × 15 cm^2) were obtained from women who had undergone a cesarean section. Chorion remnants were removed and rinsed several times with phosphate buffered saline (PBS), until no blood remained. The amniotic membrane was cut into small pieces (1–2 mm in diameter), placed in a Petri dish (Corning, Toledo, MI, USA), digested with 15 mL 0.25% trypsin (Sigma, St. Louis, MO, USA) and ethylenediamine tetraacetic acid (Sigma) for 7–8 minutes at 37°C, diluted in 100 mL PBS, and passed through a 200-mesh filter. The digestion was terminated by adding medium containing 5% fetal bovine serum (Hyclone, Logan, UT, USA), and the cell suspension was centrifuged to remove the supernatant. Following the addition of RPMI1640 medium (Gibco, Los Angeles, CA, USA) containing 10% fetal bovine serum, cells were incubated in a 5% CO_2 culture box (SPX Corporation, Charlotte, CA, USA) at 37°C. The medium was replaced completely 3 days later, and every other day thereafter. After 7–10 days, the morphology of primary cultured cells was observed by staining with cresyl violet (Chemsky International Co., Ltd., Shanghai, China) and viewing under an inverted phase contrast microscope (Olympus, Tokyo, Japan). Phenotypic markers were identified using flow cytometry and immunofluorescence 2 weeks later.

Flow cytometry

After digestion by trypsin, AECs cultured for 2 weeks *in vitro* were adjusted to a cell concentration of 1 × 10^6/mL with PBS, and incubated for 30 minutes at 4°C with the following mouse anti-human monoclonal antibodies: CD29-FITC, CD34-FITC, CD44-PE, CD45-PE, CD49d-PE, and HLA-DR-PE (Becton, Dickinson and Company, Franklin Lakes, NJ, USA). After two washes with PBS, analysis of the surface markers was performed using flow cytometry (Shikh Alsook et al., 2015) (Beckman-Coulter, Brea, CA, USA). The positive threshold was determined according to the negative control, and the positive expression rate was calculated as the number of positive cells detected/(test sample size × cell concentration).

Immunofluorescence staining

After 2 weeks in culture, a uniform layer of AECs covered the bottom of the plate. Cells were rinsed with 0.1 M PBS three times for 5 minutes each time, fixed in 4% paraformaldehyde for 30 minutes at room temperature, rinsed in PBS as before, incubated in 0.25% Triton X-100 for 15 minutes, and rinsed three times again in PBS. Nonspecific binding was blocked by incubation with normal goat serum for 30 minutes, which was then discarded and replaced, without further washes, with mouse anti-human vimentin monoclonal antibody (1:50 dilution; Santa Cruz Biotechnology, Santa Cruz, CA, USA) and mouse anti-human CK19 monoclonal antibody (1:100 dilution; Covance, Emeryville, CA, USA) for 1.5 hours at 37°C. Following three washes with PBS, cells were incubated in fluorescein isothiocyanate (FITC)-binding or tetramethyl rhodamine isothiocyanate-binding goat anti-mouse IgG (Bioworld, Dublin, OH, USA) for 1 hour at 37°C. Cells were grown in six-well culture plates, in which the slides of 1.0 × 1.0 cm^2 were placed on the bottom. Under sterile conditions, the slides were treated with poly-L-lysine. The cells began to be inoculated after drying. The slides would be removed during observation. Finally, the slides were washed and three fields were randomly selected for viewing under a fluorescence microscope (Olympus). The total number of cells was divided by the number of stained cells in each field, and a mean was taken of the three fields.

Construction of AECs and silk fibroin scaffold complexes *in vitro*

AECs harvested as described above were adjusted to a concentration of 1 × 10^6/mL, inoculated on fibroin scaffolds (Material Engineering College of Soochow University, Suzhou, China), and incubated in 24-well culture plates for 4 hours. Complete medium was added to the wells until the cells were completely submerged and fully absorbed on the scaffold. Half of the medium was replaced after 2–3 days, and cell adherence and growth were monitored daily. On day 10, the cell-scaffold complex was removed and fixed in 2.5% glutaraldehyde, washed with PBS, and dehydrated conventionally. After critical point drying and sputter-coating with gold, the complex was viewed under a scanning electron microscope.

Establishment of rat spinal cord injury model

Hemisection cavity injury models were established on the basis of the spinal cord hemisection model (Shi et al., 2014). The steps were as follows: All rats were anesthetized using 4% chloral hydrate (400 mg/kg intraperitoneally) and placed on a stereotaxic frame (RWD Life Science, Shenzhen, China). The rats were fixed in position, the fur over the thoracic spine was shaved, and the skin was sterilized. Taking T_{11} as the center, a laminectomy was performed above and below the T_{11} segment. After isolating the paravertebral muscle, the vertebral plate at the T_{11} level was removed along the T_{11-12} intervertebral space to expose the dura and form an 8 × 5 mm^2 bone window. The spinal dura mater was longitudinally cut open on the left side, under a microscope (XTL-600 microscope, Qishiwei Photoelectric Equipment Co., Ltd., Shenzhen, China) to avoid the central vein. A hemisection was performed in the spinal cord at the left T_{11} level, and the partial spinal tissue at the hemisection site was aspirated to create a cavity 3 mm in diameter. The rats lost function in their left hindlimbs immediately, and the muscular strength decreased from 21 to 0 on the Basso, Bresnahan, and Beattie (BBB) Locomotor Rating Scale (Burke, 2012). Reversible incontinence occurred at the same time. All rats received daily injections of gentamicin (10,000 units intramuscularly), and pads in their home cages were replaced twice a day. Regular bladder massage was performed to keep the perineum clean and dry.

Behavioral testing

The BBB Locomotor Rating Scale was used to assess hindlimb motor function in open field apparatus in all rats 12 hours before transplantation surgery, and 12 hours and 3, 7, 14, 21 and 28 days after surgery. A score of 21 signified normal movement, and 0 signified no movement. The observation period lasted 4 minutes. The rats received urinary bladder massage to ensure a full bladder did not influence their movement, and all rats were kept in the central area of the arena as far as possible.

Transplantation

All rats underwent transplantation surgery 1 week after model establishment.

Rats in the control group received gelatin sponges loaded with 10 μL RPMI1640 medium, which was packed into the injury cavity. A small piece of fascia was sheared to repair the dura mater, and the muscular layer and skin were sutured.

AECs were cultured for 2 weeks *in vitro*, then collected and resuspended to a final concentration of 1 × 10^6/mL (Zhu et al., 2016) for transplantation in each experimental group. Rats in the AECs group underwent similar procedures to the control group, except that cell suspension (10 μL) was added to the gelatin before being packed into the injury cavity. Silk fibroin was used as the scaffold material, which was divided into blocks of approximately 3 × 3 × 2 mm^3 on the sterile counting plate. The AECs-scaffold group received AEC suspension (10 μL; final concentration 1 × 10^6/mL) added to the scaffold, which was packed into the injury cavity. In the blank scaffold group, the same sized scaffolds were packed into the injury cavity but without AEC suspension. The muscular layer and skin were sutured, and all rats received a daily injection of gentamicin (10,000 units) for 2 weeks. Cage pads were changed twice a day, and bladder massage was performed to keep the perineal region clean and dry until independent bladder control returned.

HRP-TMB tracer

Four weeks later, all rats were anesthetized and the original incision was opened to expose the dura mater. HRP (Boster, Wuhan, China; 30%, 0.5 μL) was injected 5 mm below the primary injury with a microsample injector. The injection lasted 20 minutes with the needle at a depth of 1.5–2.0 mm, and the wound was sutured. Rats were returned to their cages and allowed to recover for 2 days.

Histochemistry of injured spinal cord

All rats were sacrificed by an overdose of anesthesia 30 days after transplantation (4 weeks plus 2 days for the neural tracing study), and then fixed with 4% paraformaldehyde. Brain and spinal cord were removed and placed in 30% sucrose at 4°C overnight. Samples were chosen from the hindlimb sensorimotor cortex, mesencephalic magnocellular red nucleus, and spinal injury and transplanted region, then permeabilized in xylene and embedded in paraffin. Tissue from different animals was cut into longitudinal and horizontal sections with a constant-temperature freezing microtome (CM1900, Leica, Germany). Sections (6 μm thick) were mounted on poly-L-lysine-coated slides, then dried and stored until use.

Tissue sections containing the transplanted area and those distal to the injury site were subjected to hematoxylin-eosin staining and immunohistochemistry against human nuclear antigen (Bioss, Beijing, China), microtubule-associated protein 2 (MAP-2) (Santa Cruz Biotechnology, Santa Cruz, CA, USA), neurofilament 200 (NF-200) (Sigma) and glial fibrillary acidic protein (GFAP) (Santa Cruz Biotechnology). The survival and differentiation of grafted AECs were then analyzed. Myelinated fiber formation in the transplanted region was evaluated. The longitudinal and transverse sections of spinal cord injury lesions and adjacent tissue were stained using the Pal-Weigert method (Sarikcioglu et al., 2001) and the Weil myelin staining kit (Shyuanmu Biotechnology, Shanghai, China) according to the manufacturer instructions. The specimens were dehydrated, permeabilized, and mounted. Continuous paraffin-embedded sections (6 μm thick) were cut in the hindlimb region of the cerebral cortex and magnocellular red nucleus, and stained with freshly prepared 3,3′,5,5′-tetramethylbenzidine (TMB) according to the manufacturer's instructions of the kit (Amresco, Rudner, Pennsylvania, USA). The number of horseradish peroxidase (HRP)-labeled neurons in the cortex and red nucleus of each group was calculated using nerve tissue shape analysis software. We collected all the paraffin sections of each animal's hindlimb region of cerebral cortex and magnocellular red nucleus. Three visual fields (BX53 microscope, Olympus, Japan) were randomly selected for cell counting at 40× magnification. The total number of TMB-stained cells in the hindlimb region of the cerebral cortex and magnocellular red nucleus in each group was calculated by dividing the total number of stained cells in each group by the number of rats.

Statistical analysis

All data are presented as the mean ± SD. Statistical analysis was performed by AHZ with SAS 9.1.1 software (SAS, Carey, CA, USA). Using a completely randomized design, a one-way analysis of variance was performed with the least significant difference *post hoc* test. A value of $P < 0.05$ was considered statistically significant.

Results

Morphological and phenotypic characteristics of AECs

Cresyl violet staining was used to reveal the morphology of the cells. Primary cells cultured for 7–10 days *in vitro* were round or polygonal in shape, with large nuclei and prominent nucleoli. Cells adhered to the wall and were in contact with each other (**Figure 1**). Flow cytometry revealed positive expression rates for CD29 and CD44 of 95.44% and 18.32%, respectively, but there was no expression of CD34, CD45, HLA-DR and CD49d. The latter was used to identify AECs (**Figure 2**). Immunofluorescence staining showed that AECs coexpressed the mesenchymal cell marker vimentin and the epithelial cell marker CK19 (**Figure 3**).

Observation of three-dimensional culture of AECs on silk fibroin scaffold *in vitro*

Under an inverted microscope and scanning electron microscope, cells planted in the scaffold for 1–2 days were found to be completely adherent. Three to five days later, the cultivated cells began to proliferate actively. Most of them extended slender processes and migrated forward along the scaffold, gradually linking into sheets within the mesh, which would later be filled with cells. On day 10, they extended uropodia and attached tightly to the scaffold with moderate extension and morphological diversity. Two to five protrusions extended from the body, some of which connected end-to-end. Cell chains were also observed, parallel or winding on the scaffold, or dangling between the roots of silk. Matrix secretions were visible on some cell bodies and scaffold (**Figure 4**). After 2 weeks, the three-dimensional scaffold began disintegrating and cells became embedded, forming a sheet-like, stretchy complex of amniotic cells and silk fibroin protein.

Hindlimb motor function

After hemisection cavity injury, the left hindlimb immediately showed a severe loss of function and the muscular strength decreased from 21 to 0 on the BBB scale. The day after surgery, all rats showed slightly restricted movements in the hindlimb contralateral to the injury, and edema and paralysis of the ipsilateral hindlimb.

One week after operation, the affected limbs of rats in the control and blank scaffold groups began to contract, but no notable contracted symptoms were found in the AECs and AECs-scaffold groups. By 2 weeks, the movement of rats in each group had markedly improved. BBB scores of the AECs-scaffold group were significantly higher than those of the other three groups ($P < 0.05$; **Table 1**).

At 4 weeks, rats in the AECs-scaffold group showed coordinated movement in the left hindlimb, and the difference in BBB scores between groups was even greater ($P < 0.05$; **Table 1**).

Immunohistochemistry

In the control group, hematoxylin-eosin staining revealed multiple foci from glial scarring within the injured site. The foci were filled with a translucent, jelly-like substance, and showed mild contraction of the axonal stump—where focal liquefaction was visible—and no axonal regeneration (**Figure 5A**). In the two AEC transplantation groups, human nuclear antigen-positive cells could be seen at the graft site, which confirmed the survival of transplanted human amniotic cells (**Figure 5B**). In the blank scaffold group, disintegrating

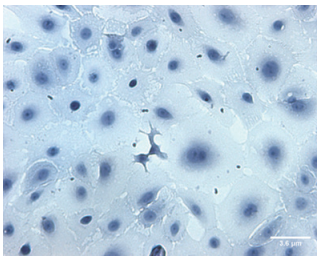

Figure 1 Human primary amniotic epithelial cells after 7–10 days in culture (cresyl violet staining, × 200).
Cells have large nuclei, prominent nucleoli, and appear round or polygonal. Amniotic epithelial cells connect with each other. Scale bar: 3.6 μm.

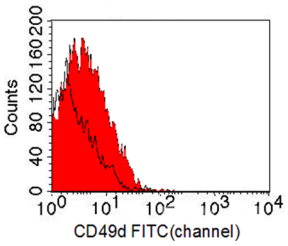

Figure 2 Negative expression of CD49d in human amniotic epithelial cells *in vitro* (flow cytometry).
The fluorescence distribution of the cells matched that of the negative control.

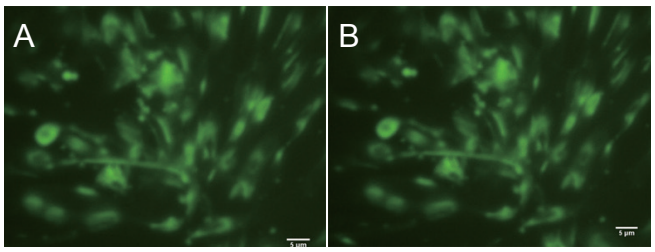

Figure 3 Coexpression of vimentin and CK19 in human amniotic epithelial cells (immunofluorescence staining; fluorescence microscope).
Amniotic epithelial cells coexpressed the mesenchymal cell marker vimentin (A) and the epithelial cell marker CK19 (B). Fluorescent agent: fluorescein isothiocyanate. Scale bars: 5 μm.

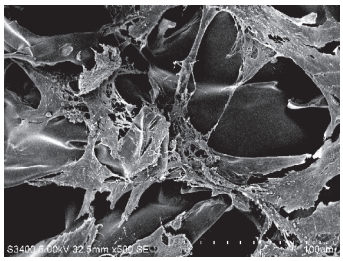

Figure 4 Morphology of human amniotic epithelial cells 1 week after implantation on the scaffold (scanning electron microscope).
One week after implantation on the scaffold, amniotic epithelial cells showed morphological diversity, multiple processes, and were stretched into a unique configuration. Scale bar: 100 μm.

Table 1 Effect of transplantation of human amniotic epithelial cells combined with silk fibroin scaffold on motor function in rats with spinal cord injury

Group	Before surgery	After surgery					
		12 hours	3 days	7 days	14 days	21 days	28 days
Control (n = 6)	21	0	2.0±0.67	2.3±0.92	3.3±1.09	4.9±0.83	5.7±1.13
AECs (n = 10)	21	0	1.8±0.63	2.8±0.79	5.0±0.81*	7.8±0.97**	10.3±1.35*
Blank scaffold (n = 6)	21	0	2.6±0.81	2.3±0.11	3.5±1.01	4.8±1.17	5.8±1.16
AECs-scaffold (n = 10)	21	0	2.4±0.94	3.4±1.03	5.8±1.22*	10.2±1.85$^{*\#}$	11.8±2.12*

Data are expressed as the mean ± SD (one-way analysis of variance and the least significant difference test). *P < 0.05, *vs.* control and blank scaffold groups; #P < 0.05, *vs.* AECs group. AECs: Amniotic epithelial cells.

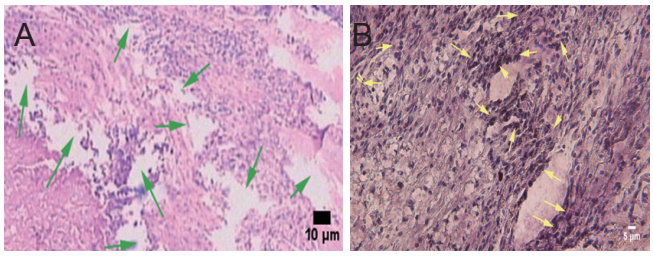

Figure 5 Effect of transplantation of human amniotic epithelial cells combined with a silk fibroin scaffold on the morphology of injured spinal cord in rats (hematoxylin-eosin staining, optical microscope).
(A) Traumatic scar in the control group, showing axonal transection, liquefaction (green arrows), and a lack of axonal regeneration. Scale bar: 10 μm. (B) Positive cells of human nuclear antigen staining in the amniotic epithelial cells group, confirming survival of transplanted cells (yellow arrows). Scale bar: 5 μm.

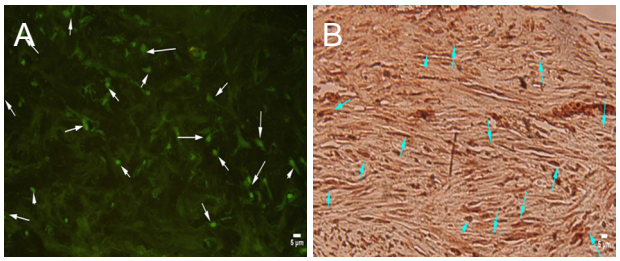

Figure 7 Effect of transplantation of human amniotic epithelial cells combined with silk fibroin scaffold on MAP-2 and NF-200 immunoreactivity in injured spinal cord of rats.
(A) MAP-2-positive cells (white arrows) in foci of the amniotic epithelial cells group, presumed to come from differentiation of amniotic epithelial cells (fluorescence microscope). (B) NF-200-positive cells (cyan arrows) in the foci of cell transplantation groups, showing good nerve repair in the lesion (optical microscope). Scale bars: 5 μm for A, B. MAP-2: Microtubule-associated protein 2; NF-200: neurofilament 200.

material filling the gaps of foci was still visible in the longitudinal section of tissue. Inflammatory cells infiltrated between the material and host tissue, and most of the lesion was filled by regenerating nerve tissue in the AECs-scaffold group. In some sections, disintegrating silk fibroin was also observed, but inflammatory cell infiltration was not seen between the material and tissue (**Figure 6**). In the two AECs transplantation groups, but not in the control and blank scaffold groups, there were MAP-2-positive cells within the lesion site (**Figure 7A**), and NF-200-positive fibers within the lesion and

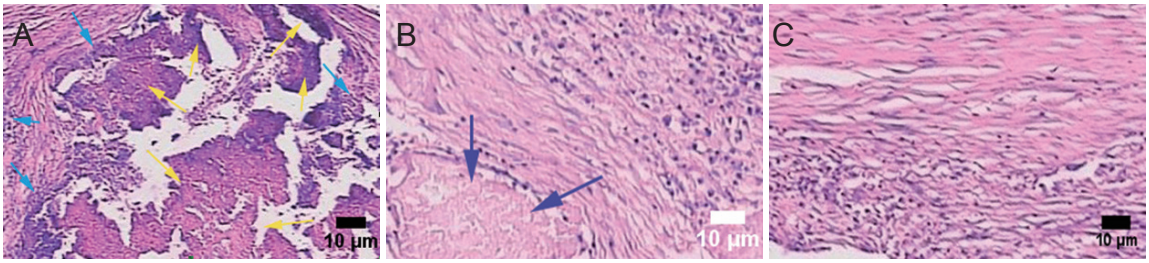

Figure 6 Effects of human amniotic epithelial cells combined with silk fibroin scaffold on the morphology of injured spinal cord (hematoxylin-eosin staining, optical microscope).
(A) In the blank scaffold group, disintegrating material (yellow arrows) filled in the injury site, and there was inflammatory cell infiltration (cyan arrows) between the material and the tissue. (B, C) Repaired nerve in the amniotic epithelial cells-scaffold group. (B) Some disintegrating materials (blue arrow) could still be found, but there was no inflammatory cell infiltration. (C) Absorption of materials in the sections. Scale bars: 10 μm.

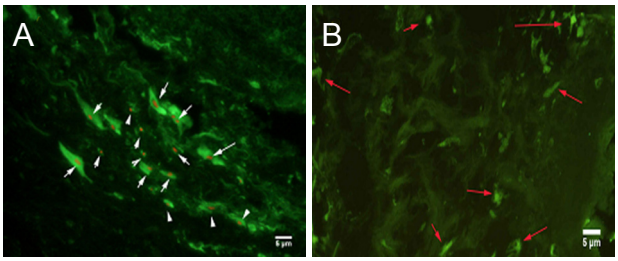

Figure 8 Effects of transplantation of human amniotic epithelial cells combined with silk fibroin scaffold on GFAP immunoreactivity in injured spinal cord tissue of rats (immunofluorescence staining, fluorescence microscope).
(A) A large number of human cell nuclear antigen and GFAP immunofluorescence double stained cells (white arrows) in the transplant area of the two cell transplantation groups. (B) In the other two groups, only a small number of GFAP-positive cells (red arrows) were found. Nuclear stain is TRITC, and cytoplasmic fluorescent agent is FITC. Scale bars: 5 μm. GFAP: Glial fibrillary acidic protein; TRITC: tetramethyl rhodamine isothiocyanate; FITC: fluorescein isothiocyanate.

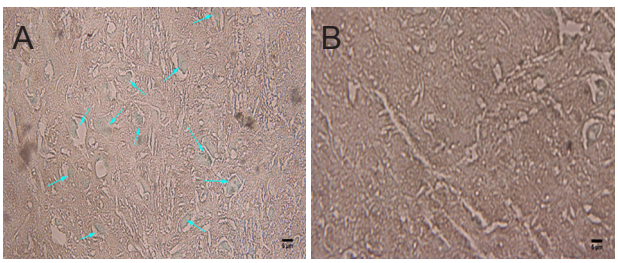

Figure 10 HRP-TMB-labeled neurons in the cortex and mesencephalic red nucleus.
(A) HRP-TMB labeled neurons (arrows) in the motor cortex and red nucleus region of rats that received transplanted cells. (B) Almost no labeled cells were found in the blank scaffold group. HRP: Horseradish peroxidase; TMB: 3,3′,5,5′-tetramethylbenzidine. Scale bars: 5 μm.

distal tissues of the spinal cord (**Figure 7B**). Double immunofluorescence labeling of human cell nuclear antigen and GFAP within the transplanted area showed a large number of double-stained cells in both cell transplantation groups, confirming the survival of the transplanted cells in the host (**Figure 8A**). In the other two groups, only a few GFAP-positive cells (red arrows) were found (**Figure 8B**). One month after transplantation, Pal-Weigert staining near injured foci of each group showed only a few myelinated fibers in the control group and blank scaffold group; in contrast, a large number of myelinated fibers were visible in the transplanted

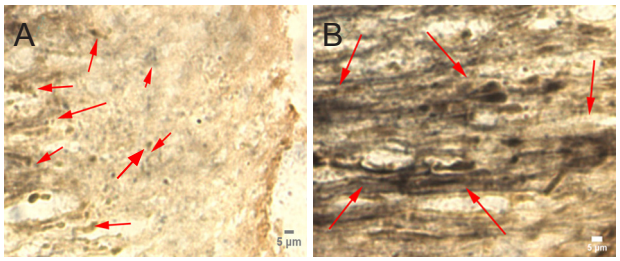

Figure 9 Effects of transplantation of human amniotic epithelial cells combined with silk fibroin scaffold on the myelin morphology of injured spinal cord in rats (Pal-Weigert staining, optical microscope).
(A) One month after transplantation, a small number of stained fibers (black fibers; red arrows) were seen in cross-sectional slices of the control and blank scaffold groups. (B) In contrast, a large number of myelinated fibers (black fibers; red arrows) were seen in the transplanted area of the two cell transplantation groups. Scale bars: 5 μm.

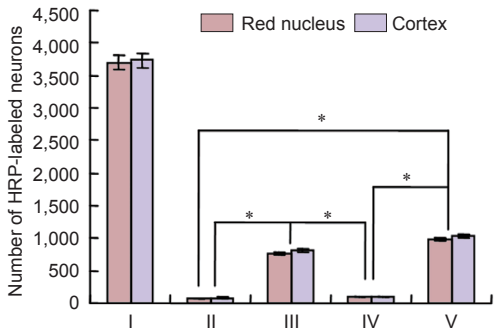

Figure 11 Quantification of HRP-TMB-labeled neurons in the cortex and mesencephalic red nucleus of different groups, measured with the HRP-TMB tracer technique.
There were significant differences in the total number of neurons between cell transplantation groups (III, V) and non cell transplantation groups (II, IV) (*$P < 0.05$; mean ± SD, one-way analysis of variance and least significant difference test). I: Normal side; II: control group ($n = 6$); III: amniotic epithelial cells group ($n = 6$); IV: blank scaffold group ($n = 10$); V: amniotic epithelial cells-scaffold group ($n = 10$). HRP: Horseradish peroxidase; TMB: 3,3′,5,5′-tetramethylbenzidine.

area in the two cell transplantation groups (**Figure 9**).

Quantitative analysis of labeled neurons in the cortex and mesencephalic red nucleus with HRP-TMB tracer technique

HRP-TMB labeling was used to examine the effect of the grafts on nerve repair. HRP-labeled neurons on the side con-

tralateral to the injury were mainly located in the ventrolateral part of the red nucleus and cortical motor area. Neurons on the side ipsilateral to the injury were hardly labeled by HRP in the control and blank scaffold groups. More labeled neurons could be seen in the AECs-scaffold group than in the AECs group ($P < 0.05$). The number of labeled neurons in the two cell transplantation groups was significantly higher than in the two groups that did not receive transplanted cells ($P < 0.05$; **Figures 10**, **11**).

Discussion

The mechanisms underlying spinal cord injury and axonal regeneration, especially late recovery from complete spinal cord injury, are of great interest to neuroscience researchers. Conventional research suggested that no treatment could restore neurological loss. However, over the past 20 years, cell transplantation has emerged as a promising means of treating central nervous system disorders such as spinal cord injury. The transplanted cells act as a source of nerve growth factor, help damaged cells survive, and secrete other factors to confront the inhibitory action caused by excessive activation of glial cells, thus repairing damaged neural pathways and restoring function. The use of human AECs as seed cells is gaining increasing research attention.

Embryologically, both AECs and nerve cells originate from a morula, an ectodermal cell mass that can differentiate into various tissues and organs. Because the amniotic membrane is an early product of embryonic development, there is reason to believe that AECs are a kind of pluripotent stem cell. Some studies have also shown that AECs are good materials for cell transplantation (Broughton, et al., 2013; Rutigliano et al., 2013; Barboni et al., 2014). Compared with other candidates, AECs are more accessible, less immunogenic, and have the immune regulation characteristics of mesenchymal cells (Wu et al., 2014). They are one of the most likely seed cell types to enter clinical research.

Our experiment has shown that cultured AECs express a variety of stem cell markers in culture, and MAP, NF, and myelin markers in the host environment after transplantation. We also confirmed that AECs could survive and integrate with the host 1 month after transplantation. Lesions were completely filled by the transplanted cells and proliferating glial cells, without any cysts or obvious scars.

Pal-Weigert staining revealed a large number of myelinated fibers in the graft-host interface in the two groups that received the transplant, but only a few stained fibers were observed in the control and blank scaffold groups. We could not distinguish whether these fibers came from the severed corticospinal tract or the regenerated rubrospinal tract. A study by Wu et al. (2009) indicated that these two tracts have different regeneration capacities: the corticospinal tract only grew in the matrix environment provided by gray matter due to its slightly weaker regenerative capacity, whereas the rubrospinal tract had such strong regeneration ability that it could regenerate in the white matter environment and in a variety of transplant environments. However, our HRP retrograde labeling experiment did not show a significant difference between the numbers of the two kinds of regenerative nerve fibers.

The AECs-scaffold group showed excellent potential for nerve repair in the present study. Silk fibroin is the main component of silk, which can support cell adhesion, differentiation and tissue formation, and was shown not to cause a T-cell-mediated response *in vivo*. With good cell adhesion properties, and maintenance of normal cellular morphology and function, it is a natural scaffold for three-dimensional culture (Luan et al., 2009). Compared with the artificial scaffold materials more frequently used in experimental studies (Wang et al., 2011; Shahriari et al., 2015; Oprych et al., 2016), silk fibroin has better biocompatibility, and its biodegradation is more closely matched to that of the repair process.

In the present study, the complexes constructed by amniotic cells and silk fibroin protein showed that cells on the surface of the material had sufficient adsorption capacity *in vitro* and *in vivo*. Its excellent biocompatibility ensured that transplanted cells have a three-dimensional porous growth surface, which greatly enhances the surface area of cell growth, and promotes cell adherence, immobilization and propagation, in line with cell survival. Our experimental results also supported the theory that seed cell transplantation with tissue engineering could be more conducive to regeneration and repair of damaged nerve tissue than single cell transplantation. The scaffold provided a more favorable environment for the regeneration of the central nervous system. The experiment also confirmed that the silk fibroin scaffold has an appropriate biodegradation rate, allowing it to be gradually absorbed, and eventually disappear, as the tissue regenerates; this is necessary in the ideal tissue-engineered scaffold.

Biopsy tissue from graft sites of the blank scaffold group showed that there was a lot of inflammatory cell infiltration in the graft-host interface, indicating that the host still had a degree of foreign body rejection against this material, but the same response was rarely observed in the AECs-scaffold group. This might be due to the immunosuppressive and immunomodulatory properties of amniotic cells (Barboni et al., 2014), so that the two graft materials complement each other. Further research is needed to clarify the complex molecular mechanisms underlying recovery after spinal cord injury.

Acknowledgments: *The authors gratefully acknowledge the help of all volunteers (Brain Research Institute of the First Affiliated Hospital, Soochow University, China; Cell Research Institute of Wuxi Third People's Hospital, China) who participated in this study.*
Author contributions: *GZH and WJW designed the study. TGW, PZ and ZNM performed experiments. JX and AHZ analyzed data and made statistical analysis. HL and WJW provided critical revision of the manuscript for intellectual content. TGW wrote the paper. PZ provided fund support. All authors approved the final version of the paper.*
Conflicts of interest: *None declared.*
Plagiarism check: *This paper was screened twice using CrossCheck to verify originality before publication.*
Peer review: *This paper was double-blinded and stringently reviewed by international expert reviewers.*

References

Arkhipova AY, Kotlyarova MC, Novichkova SG, Agapova OI, Kulikov DA, Kulikov AV, Drutskaya MS, Agapov II, Moisenovich MM (2016) New silk fibroin-based bioresorbable microcarriers. Bull Exp Biol Med 160:491-494.

Barboni B, Russo V, Curini V, Martelli A, Berardinelli P, Mauro A, Mattioli M, Marchisio M, Bonassi Signoroni P, Parolini O, Colosimo A (2014) Gestational stage affects amniotic epithelial cells phenotype, methylation status, immunomodulatory and stemness properties. Stem Cell Rev 10:725-741.

Binan L, Tendey C, De Crescenzo G, El Ayoubi R, Ajji A, Jolicoeur M (2014) Differentiation of neuronal stem cells into motor neurons using electrospun poly-L-lactic acid/gelatinscaffold. Biomaterials 35:664-674.

Broughton BR, Lim R, Arumugam TV, Drummond GR, Wallace EM, Sobey CG (2013) Post-stroke inflammation and the potential efficacy of novel stem cell therapies: focus on amnion epithelial cells. Front Cell Neurosci 6:66.

Burke DA, Magnuson DS (2012) Basso, Beattie, and Bresnahan scale locomotor assessment following spinal cord injury and its utility as a criterion for other assessments. Animal Models of Acute Neurological Injuries II. Springer Protocols Handbooks 2:591-604.

Chow WN, Simpson DG, Bigbee JW, Colello RJ (2007) Evaluating neuronal and glial growth on electrospun polarized matrices: bridging the gap in percussive spinal cord injuries. Neuron Glia Biol 3:119-126.

Corradetti B, Meucci A, Bizzaro D, Cremonesi F, Lange Consiglio A (2013) Mesenchymal stem cells from amnion and amniotic fluid in the bovine. Reproduction 145:391-400.

Council for International Organizations of Medical Sciences (2002) International ethical guidelines for biomedical research involving human subjects. Bull Med Ethics 17-23.

Dingle YT, Boutin ME, Chirila AM, Livi LL, Labriola NR, Jakubek LM, Morgan JR, Darling EM, Kauer JA, Hoffman-Kim D (2015) Three-dimensional neural spheroid culture: an in vitro model for cortical studies. Tissue Eng Part C Methods 21:1274-1283.

Gao Y, Pu Y, Wang D, Hou L, Guan W, Ma Y (2012) Isolation and biological characterization of chicken amnion epithelial cells. Eur J Histochem 56:208-214.

Ghezzi CE, Marelli B, Muja N, Hirota N, Martin JG, Barralet JE, Alessandrino A, Freddi G, Nazhat SN (2011) Mesenchymal stem cell-seeded multilayered dense collagen-silk fibroin hybrid for tissue engineering applications. Biotechnol J 6:1198-1207.

Gramignoli R, Srinivasan RC, Kannisto K, Strom SC (2016) Isolation of human amnion epithelial cells according to current good manufacturing procedures. Curr Protoc Stem Cell Biol 37:1E.10.1-1E.10.13.

Hopkins AM, DeSimone E, Chwalek K, Kaplan DL (2015) 3D in vitro modeling of the central nervous system. Prog Neurobiol 125:1-25.

Hsieh FY, Hsu SH (2015) 3D bioprinting: a new insight into the therapeutic strategy of neural tissueregeneration. Organogenesis 11:153-158.

Jgamadze D, Liu L, Vogler S,Chu LY, Pautot S (2015) Thermoswitching microgel carriers improve neuronal cell growth and cell release for cell transplantation. Tissue Eng Part C Methods 21:65-76.

Karumbaiah L, Enam SF, Brown AC, Saxena T, Betancur MI, Barker TH, Bellamkonda RV (2015) Chondroitin sulfate glycosaminoglycan hydrogels create endogenous niches for neural stem cells. Bioconjug Chem 26:2336-2249.

Khankan RR, Wanner IB, Phelps PE.(2015) Olfactory ensheathing cell-neurite alignment enhances neurite outgrowth in scar-like cultures. Exp Neurol 269:93-101.

Lee-Liu D, Edwards-Faret G, Tapia VS, Larraín J (2015) Spinal cord regeneration: lessons for mammals from non-mammalian vertebrates. Genesis 51:529-544.

Li H, Ham TR, Neill N,Farrag M, Mohrman AE, Koenig AM, Leipzig ND (2016) A hydrogel bridge incorporating immobilized growth factors and neural stem/progenitor cells to treat spinal cord injury. Adv Healthc Mater doi: 10.1002/adhm.201500810.

Luan XY, Huo GH, Li MZ, Lu SZ, Zhang XG (2009) Antheraea pernyi silk fibroin maintains the immunosupressive properties of human bone marrow mesenchymal stem cells. Cell Biol Int 33:1127-1134.

Marsano E, Corsini P, Canetti M, Freddi G (2008) Regenerated cellulose-silk fibroin blends fibers. Int J Biol Macromol 43:106-114.

Meinel L, Hofmann S, Karageorgiou V, Kirker-Head C, McCool J, Gronowicz G, Zichner L, Langer R, Vunjak-Novakovic G, Kaplan DL (2005) The inflammatory responses to silk films in vitro and in vivo. Biomaterials 26:147-155.

Min SK, Jung SM, Ju JH, Kwon YS, Yoon GH, Shin HS (2015) Regulation of astrocyte activity via control over stiffness of cellulose acetate electrospun nanofiber. In Vitro Cell Dev Biol Anim 51:933-940.

Oprych KM, Whitby RL, Mikhalovsky SV, Tomlins P, Adu J (2016) repairing peripheral nerves: is there a role for carbon nanotubes? Adv Healthc Mater doi: 10.1002/adhm.201500864.

Rivet CJ, Zhou K, Gilbert RJ, Finkelstein DI, Forsythe JS (2015) Cell infiltration into a 3D electrospun fiber and hydrogel hybrid scaffold implanted in the brain. Biomatter 5:e1005527.

Rutigliano L, Corradetti B, Valentini L (2013) Molecular characterization and in vitro differentiation of feline progenitor-like amnioticepithelial cells. Stem Cell Res Ther 4:133.

Sarikcioglu L, Oguz N (2001) Exercise training and axonal regeneration after sciatic nerve injury. Int J Neurosci 109:173-177.

Shahriari D, Koffler J, Lynam DA, Tuszynski MH, Sakamoto JS (2015) Characterizing the degradation of alginate hydrogel for use in multilumen scaffolds for spinal cord Repair. J Biomed Mater Res A doi: 10.1002/jbm.a.35600.

Shi Q, Gao W, Han X, Zhu X, Sun J, Xie F, Hou X, Yang H, Dai J, Chen L (2014) Collagen scaffolds modified with collagen-binding bFGF promotes the neural regeneration in a rat hemisected spinal cord injury model. Sci China Life Sci 57:232-240.

Shikh Alsook MK, Gabriel A, Piret J, Waroux O, Tonus C, Connan D, Baise E, Antoine N (2015) Tissues from equine cadaver ligaments up to 72 hours of post-mortem: a promising reservoir of stem cells. Stem Cell Res Ther 6:253.

Tang X, Ding F, Yang Y, Hu N, Wu H, Gu X (2009) Evaluation on in vitro biocompatibility of silk fibroin-based biomaterials with primarily cultured hippocampal neurons. J Biomed Mater Res A 91:166-174.

Taylor AC, Vagaska B, Edgington R, Hébert C, Ferretti P, Bergonzo P, Jackman RB (2015) Biocompatibility of nanostructured boron doped diamond for the attachment and proliferation of human neural stem cells. J Neural Eng 12:066016.

van Neerven SG, Krings L, Haastert-Talini K, Vogt M, Tolba RH, Brook G, Pallua N, Bozkurt A (2014) Human Schwann cells seeded on a novel collagen-based microstructured nerve guide survive, proliferate, and modify neurite outgrowth. Biomed Res Int 2014:493823.

Wang J, Zheng J, Zheng Q, Wu Y, Wu B, Huang S, Fang W, Guo X (2015) FGL-functionalized self-assembling nanofiber hydrogel as a scaffold for spinal cord-derived neural stem cells. Mater Sci Eng C Mater Biol Appl 46:140-7.

Wang M, Zhai P, Chen X (2011) Bioengineered scaffolds for spinal cord repair. Tissue Eng Part B Rev 17:177-194.

Woloszyk A, Liccardo D, Mitsiadis TA (2016) Three-dimensional imaging of the developing vasculature within stem cell-seeded scaffolds cultured in ovo. Front Physiol 7:146.

Wu D, Yang P, Zhang X, Luo J, Haque ME, Yeh J, Richardson PM, Zhang Y, Bo X (2009) Targeting a dominant negative rho kinase to neurons promotes axonal outgrowth and partial functional recovery after rat rubrospinal tract lesion. Mol Ther 17:2020-2030.

Wu WJ, Lan Q , Lu H, Xu J, Zhu A, Fang W, Ge F, Hui G (2014) Human amnion mesenchymal cells negative co-stimulatory molecules PD-L1 expression and its capacity of modulating microglial activation of CNS. Cell Biochem Biophys 69:35-45.

Zhao Y, Zhao W, Yu S, Guo Y, Gu X, Yang Y (2013) Biocompatibility evaluation of electrospun silk fibroin nanofibrous mats with primarily cultured rat hippocampal neurons. Biomed Mater Eng 23:545-554.

Zhu D, Muljadi R, Chan ST, Vosdoganes P, Lo C, Mockler JC, Wallace EM, Lim R (2016) Evaluating the impact of human amnion epithelial cells on angiogenesis. Stem Cells Int 2016:1-13.

Zhu T, Tang Q, Shen Y, Tang H, Chen L, Zhu J (2015) An acellular cerebellar biological scaffold: Preparation, characterization, biocompatibility and effects on neural stem cells. Brain Res Bull 113:48-57.

Copyedited by Slone-Murphy J, Stow A, Wang J, Qiu Y, Li CH, Song LP, Zhao M